Analysis of the impact of surface layer parameters on wear intensity of friction pairs

R. Burdzik*, P. Folęga, B. Łazarz, Z. Stanik, J. Warczek

Faculty of Transport, Silesian University of Technology,
ul. Krasińskiego 8, 40-019 Katowice, Poland
* Corresponding e-mail address: rafal.burdzik@polsl.pl

ABSTRACT

Purpose: The study discussed in the paper consisted in testing the impact of surface layer parameters on wear intensity of friction pair components. The study was conducted having taken additional operational factors into consideration, namely the friction conditions (presence of lubricant) and the value of loads affecting the contact zone of the samples being tested.

Design/methodology/approach: The study constituted laboratory tests of wear and were conducted by means of a T-01M type laboratory test stand used to experimentally analyse frictional cooperation of various materials used in structural components of motor vehicles. The friction pairs examined were previously operating in a pin-on-disk system under various conditions. The materials of the friction pairs tested at the stand were subjected to heat treatment and chemical processing in order to attain specific parameters of their surface layers.

Findings: The studies conducted enabled determination of the abrasive wear values for the material samples tested having entailed the surface layer parameters and the factors related to operation of actual structural components used in automotive engineering. An additional advantage of the studies conducted was the possibility to establish actual coefficients of friction occurring in specific friction pairs.

Research limitations/implications: Establishing the actual values of friction coefficients for the materials of friction pairs under specific conditions and having taken the impact of the surface layer parameters into consideration enabled identification of the reasons for excessive surface wear. Hence a reference can be made between the stationary tests undertaken and actual components cooperating with one another in kinematic pairs of machines.

Originality/value: The utilitarian premise resulting from the studies conducted is the necessity of paying particular attention to surface layer parameters while designing friction pairs for machines.

Keywords: Surface layer; Wear; Friction coefficient

Reference to this paper should be given in the following way:

R. Burdzik, P. Folęga, B. Łazarz, Z. Stanik, J. Warczek, Analysis of the impact of surface layer parameters on wear intensity of friction pairs, Archives of Materials Science and Engineering 58/2 (2012) 146-151.

METHODOLOGY OF RESEARCH, ANALYSIS AND MODELLING

1. Introduction

An inherent aspect of machinery operation is the wearing process of individual components. Its final effects are particularly noticeable in components of friction pairs. Durability of friction pair components may be determined based on an analysis of their progressing wear. It is defined as gradual deterioration understood as the components losing their service properties. The reasons for wear may vary and they include external input functions as well

as physical and chemical factors affecting them throughout the entire period of their components' service lives [1,2,5]. Measures of wear are expressed in the appropriate units, e.g. length (linear wear), volume (volumetric wear) or mass (mass wear). In paper [8] the application of vibration method for materials properties research were presented. It can be used the measurement system described in [9]. When machine components are serviced in an appropriate manner, their wear is usually of small intensity and their service life is sufficiently long. However, operational practice shows examples of cases when accelerated wear of friction pair components is not caused by operational faults.

Excessive wear of component surfaces may result from reasons related to material or technological factors [3,4,6].

Studies of excessively worn-out components of real friction pairs have enabled various hypotheses to be proposed with regard to the reasons for their excessive wear. However, they have not made it possible to determine the impact of the said factors on the wear intensity, and hence on the occurrence of accelerated wear cases as well. This is due to the fact that conditions under which the individual components operate are not known. It is therefore substantial that laboratory tests of wear should be conducted in a manner enabling determination of these conditions. Results of such studies will lead to establishing correlations between wear intensity and the individual factors.

2. Subject and methodology of the study

The laboratory tests conducted under the study comprised assessment of wear and metallographic observations. The laboratory wear tests were conducted using the T-01M type test stand configured to operate in a pin-on-disk system. Its diagram has been provided in Fig. 1.
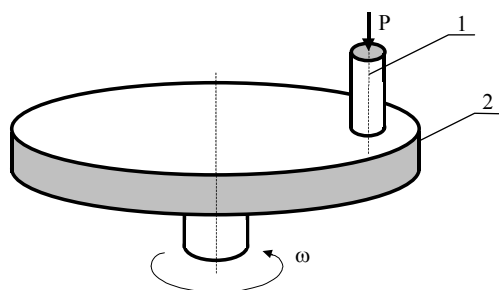

Fig. 1. Diagram of a T01M test stand, 1 - sample, 2 - countersample, P - force, ω - countersample's angular velocity

The sample used in the study has been depicted in Fig. 8. It was a cylinder of the diameter of 8 mm the end of which was a pin of the diameter of 3 mm ended with a spherical surface of the radius of 1.5 mm. Using such a shape of the sample's end enabled attaining pressures comparable to those occurring during standard operation as well as excessive pressure of the surface of cooperating components which may be due to such aspects as structural defects.

Components of a friction pair, i.e. the sample and the countersample, were made of the same cast iron grades as those used to manufacture friction pair components for motor vehicles, e.g. camshafts and followers for combustion engines. The samples

were made of type Gh 90-52-05 nodular cats iron the chemical composition of which has been provided in Table 1.

Samples made of the materials also forming the friction pair examined, after being polished and etched in nital, were observed by applying microscopic techniques. The assessment of the surface layer structure was conducted for samples made of the Gh 90-52-05 cast iron after their heat treatment as well as chilled countersamples made of the GhW1m cast iron, and it also applied to the structure of non-processed areas of samples.

Table 1.
Chemical composition of the Gh 90-52-05 cast iron (FIAT standard no. 52215)

Symbol	Chemical composition [%]								
	C	Si	Mn	Mg	S	P	Cr	Ni	Mo
Gh 90-52-05	3.7	2.65	0.2	0.01-0.05	$\leq$ 0.015	$\leq$ 0.05	-	0.40	-

Characteristic structures observed in surface layers of the samples have been depicted in Figs. 2, 3, 4 and 5, where one can clearly notice modular graphite in a martensitic and pearlitic matrix.
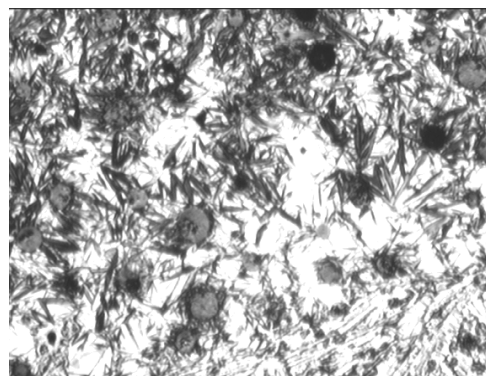

Fig. 2. Surface layer structure. Visible modular graphite in a martensitic matrix. Etched in nital, magnification of 200x, optical microscope
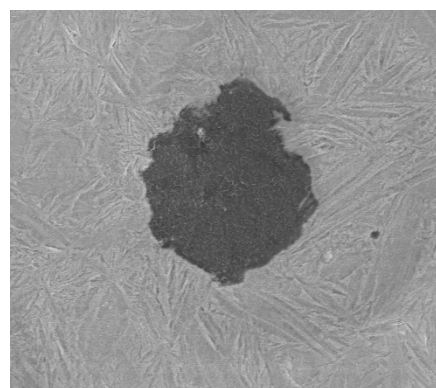

Fig. 3. Surface layer structure of a undamaged cam. Visible modular graphite in a martensitic matrix. Etched in nital, magnification of 1500x, scanning microscope
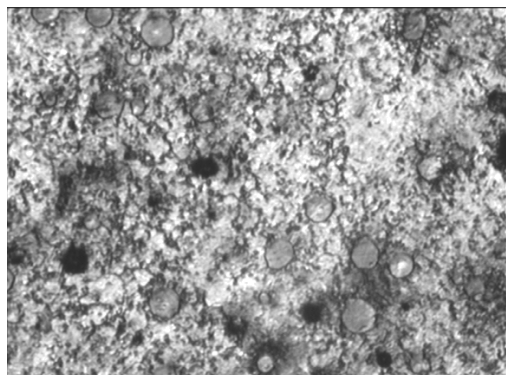
Fig. 4. Surface layer structure of a cam. Visible modular graphite in a pearlitic matrix. Etched in nital, magnification of 200x, optical microscope
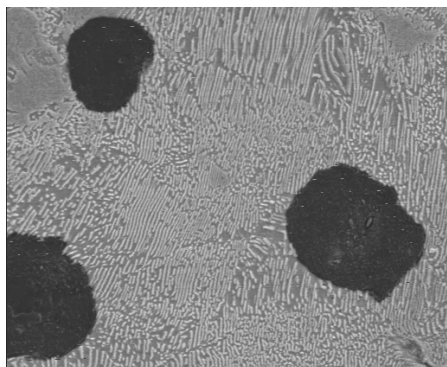

Fig. 5. Surface layer structure of a undamaged cam. Visible modular graphite in a pearlitic matrix. Etched in nital, magnification of 1,500x, scanning microscope

The structure of the areas outside the surface layer was typically that of nodular cast iron with modular graphite in a pearlitic matrix (Fig. 6). In the transition zone, one could observe small traces of a eutectic structure emerging from the side of the heat treated layer (Fig. 7).
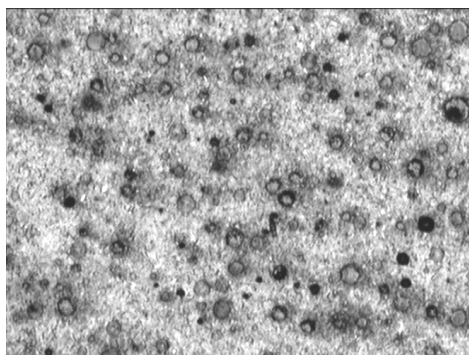

Fig. 6. Cam's structure under the surface layer. Visible modular graphite in a pearlitic matrix. Etched in nital, magnification of 200x
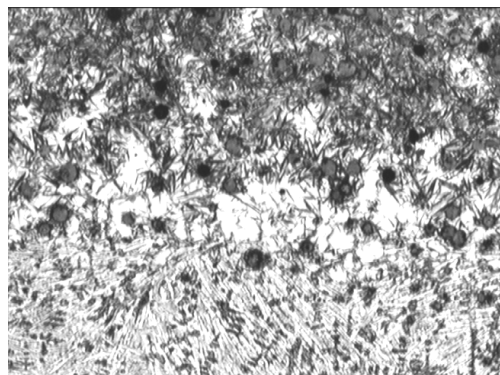

Fig. 7. Cam's structure in the transition zone between the processed surface layer and the core. Visible modular graphite in a pearlitic matrix from the core side and a eutectic structure from the surface layer side. Etched in nital, magnification of 200x

The stationary tests were conducted using the T01M device assuming different values of the cast iron hardness. It was quenched to obtain hardness parameters of the values in three ranges: 37-38 HRC, 43-44 HRC and 53-55 HRC. The geometrical form of the sample used in the tests has been depicted in Fig. 8.
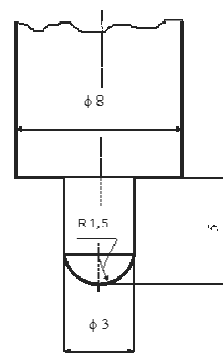

Fig. 8. Sample used in laboratory wear tests

The countersamples were made of the GhW1m cast iron. Characteristic structures observed in the surface layer have been depicted in Fig. 9.
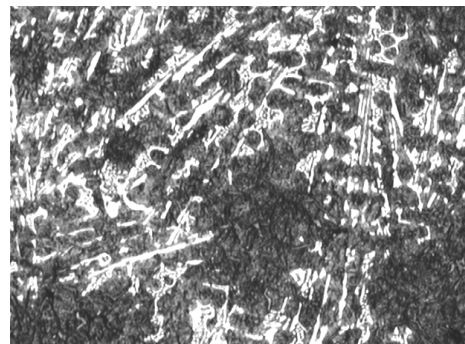

Fig. 9. Chilled layer structure of a follower. Visible martensite, cementite and graphite. Etched in nital, magnification of 100x

The countersamples tested were previously quenched to obtain the hardness of 46-48 HRC. Their form was that of a ring of the internal diameter of 40 mm and the thickness of 3 mm (Fig. 10).
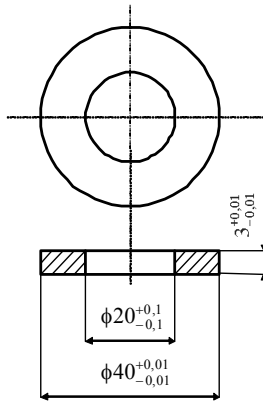
Fig. 10. Countersample used in laboratory wear tests

The tests were conducted on the load of P = 49.05 N under the conditions of dry friction as well as on lubrication with class SG/CD 15W/40 engine oil. Since the load was decreasing during the tests as a result of the sample wear, the friction distance was to be chosen in a manner ensuring that the load changes were not too large. This choice was made during preliminary studies. The proper dry wear tests were conducted at the rubbing velocity of the countersample and the sample equalling 1 m/s. In tests with lubrication, the rubbing velocity came to 0.5, 1, 1.5 and 2 m/s. Due to small material decrements occurring during the tests in presence of oil, one could not apply direct linear or mass measurement. The measurements consisted in establishing the contact area by means of a visual system cooperating with a computer. After each cycle of tests, a photograph of the sample end with traces of wear was taken. The image of the sample wear traces recorded in a digital form was subject to further analysis enabling each time the areas of the wear traces to be calculated. Assuming that the wear trace formed a circle, and the sample ends were hemispheres, the linear wear of a sample was calculated according to the following formula:

$$Z = R - \sqrt{R^2 - r^2} \tag{1}$$

where: Z - linear wear, R - radius of the spherical sample end, r - radius of the circle forming the wear trace:

$$r = \sqrt{\frac{S}{\pi}} \tag{2}$$

where: S - wear trace area.

The T01M test stand was equipped with a friction force sensor and a dedicated system for its automatic recording. The friction force parameter was applied to determine the friction coefficient. A sample course of the friction coefficient obtained during the dry friction tests (Fig. 11) has been depicted in Fig. 1, whereas Fig. 12 shows the same measure on friction with oil.
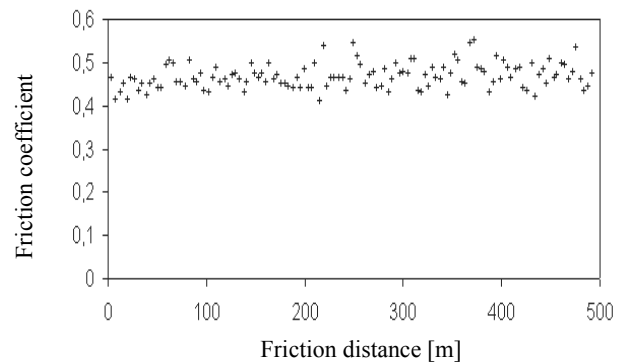
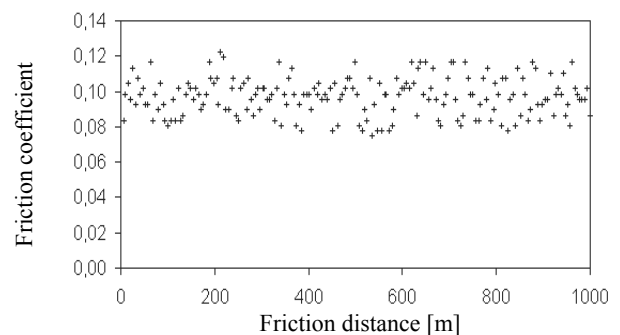Fig. 11. Course of friction coefficient during a sample wear test on dry friction

Fig. 12. Course of friction coefficient during a sample wear test on oil lubrication

The analysis of the diagrams drawn up for the friction coefficient obtained during the tests implies that its value varies is subject to variations around a specific constant. Therefore, for each test result a mean friction coefficient was calculated. In order to minimise the impact of geometrical errors in the fabrication of the components examined on the results obtained, prior to measurement series, each sample and countersample was subject to running-in.

3. Abrasive wear assessment of kinematic pairs

The results obtained in the study for linear sample wear assumed values from a very wide range, particularly in the case of frictional cooperation of the components in question in presence of a lubricant. Therefore, for the sake of further analysis, a measure in the form of linear wear intensity was applied. The laboratory test results obtained for abrasive wear of the materials examined have been depicted in Figs. 13 and 14.

The linear wear intensity of I samples is a correlation between their linear wear increment ΔZ and friction distance increment Δl:

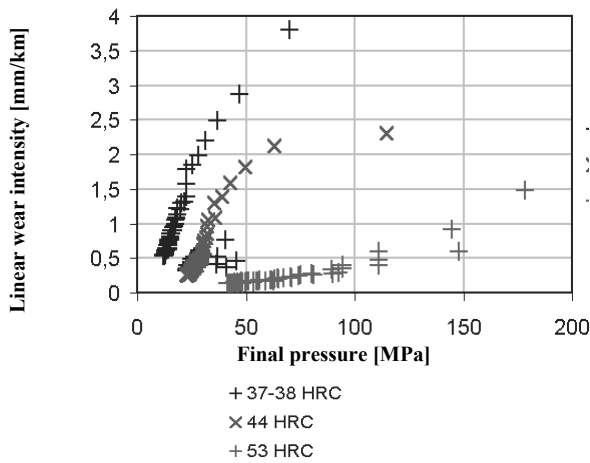$$I = \frac{\Delta Z}{\Delta l} \tag{3}$$

Fig. 13. Linear wear intensity of samples in the function of pressure for dry friction
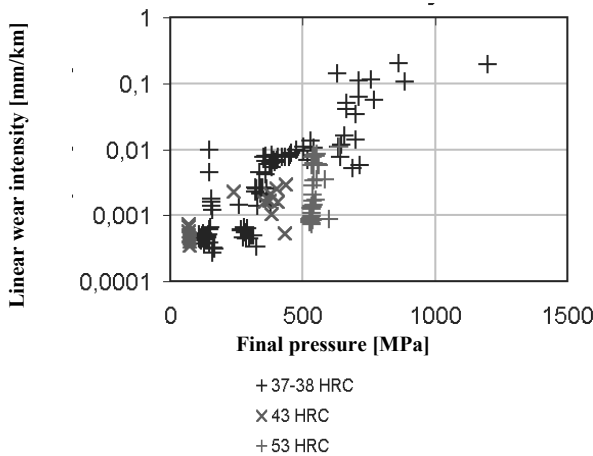

Fig. 14. Linear wear intensity of samples in the function of pressure for friction in presence of a lubricant

Applying the wear intensity measure enables synthetic representation of the test results based on a small number of diagrams.

In the course of the laboratory tests of abrasive wear, linear wear intensity of samples made of nodular cast iron was determined for different operating conditions and material hardness values. The results obtained enable establishing the correlation between wear intensity and the factors altered while testing. Before the model was prepared, individual quantities decisive for the wear of components of the friction pair studied were chosen. The material factors taken into consideration comprised hardness values of the sample and the countersample. The quantities chosen to characterise the operating conditions of the friction pair comprising the sample and the countersample were as follows:

- maximum Hertz pressure p_0;
- rubbing velocity v;
- friction distance l, also referred to as rubbing distance,
- friction coefficient μ.

The model assumed the following function to take effect:

$$Z = f(p_0, H_1, H_2, l, v, \mu),\tag{4}$$

where:
Z - linear wear being a liner decrement of the specimen or cam dimension in m,
p_0 - maximum Hertz pressure at the contact surface in Pa (kg m^{-1} s^{-2}),
H_1, H_2 - hardness of friction pair components (the examined and the cooperating one accordingly),
l - friction distance in m,
v - rubbing velocity in m/s,
μ - friction coefficient.

Since there are three dimensions in the quantities present in the above formula (no. 1), i.e. mass, length and time, hence in accordance with the principles of dimensional analysis, three base quantities were chosen to express the remaining quantities. They were: l, v and H_1.

By applying these quantities, the function given by formula (1) was transformed to assume the following form:

$$F(K_1, K_2, K_3, K_4) = 0\tag{5}$$

where: variables K_i are dimensionless products containing base quantities raised to the power of a_{ij} and each one of the remaining first power quantities:

$$K_1 = Z \cdot l^{a_{11}} \cdot v^{a_{12}} \cdot H_1^{a_{13}}, \quad K_2 = p_0 \cdot l^{a_{21}} \cdot v^{a_{22}} \cdot H_1^{a_{23}}$$
$$K_3 = H_2 \cdot l^{a_{31}} \cdot v^{a_{32}} \cdot H_1^{a_{33}}, \quad K_4 = \mu \cdot l^{a_{41}} \cdot v^{a_{42}} \cdot H_1^{a_{43}}$$

Exponents a_{ij} were calculated in the following manner:
Dimension K_1 equals:

$$[K_1] = m \cdot (m)^{a_{11}} \cdot (m \cdot s^{-1})^{a_{12}} \cdot (m^{-1} \cdot s^{-2} \cdot kg)^{a_{13}}\tag{6}$$

Since quantity K_1 is dimensionless, exponent a_{ij} should be chosen in a manner ensuring that the total exponent for each dimension equals zero.
And hence accordingly:

for [m] $0 = 1 + a_{11} + a_{12} - a_{13}$
for [s] $0 = - a_{12} - 2a_{13}$
for [kg] $0 = a_{13}$

The foregoing implies that:

$$a_{13} = 0, \ a_{12} = 0, \ a_{11} = -1$$

Therefore:

$$K_1 = Z \cdot l^1 \cdot v^0 \cdot H_1^0 = \frac{Z}{l}\tag{7}$$

The remaining K quantities were established accordingly.

$$K_2 = \frac{p_0}{H_1}, K_3 = \frac{H_2}{H_1}, K_4 = \mu \tag{8}$$

It was possible to establish linear wear intensity based on the model owing to the following form it took:

$$\frac{Z}{l} = f\left(\frac{p_0}{H_1}, \frac{H_2}{H_1}, \mu\right) \tag{9}$$

According to the recommendations provided in paper [5], the following mathematical form of function (9) was assumed:

$$\frac{Z}{l} = a_0 \left(\frac{p_0}{H_1}\right)^{a_1} \left(\frac{H_2}{H_1}\right)^{a_2} \mu^{a_3} \tag{10}$$

where: a_0, a_1, a_2, a_3 were coefficients established by regression of the laboratory wear test results.

The above function was transformed into a linear function by finding logarithms for both sides of equation (10). It enabled using the linear regression to determine coefficients a_i.

Average values of these coefficients along with standard deviations have been provided in Table 2. The table also contains values of probability that the individual coefficients equal 0. The quality of the regression performed was determined using a square of the R^2 correlation coefficient.

Table 2.
Wear model coefficients and R^2

Coefficient a_i	Mean value	Standard deviation	Probability that coefficient a_i equals 0
$\ln a_0$	-11.39	0.36	$7.67 \cdot 10^{-99}$
a_0	$1.13 \cdot 10^{-5}$	-	-
a_1	1.00	0.11	$1.93 \cdot 10^{-17}$
a_2	2.69	0.42	$6.60 \cdot 10^{-10}$
a_3	3.23	0.13	$2.56 \cdot 10^{-79}$
R^2	0.80	-	-

The R^2 value obtained was high (it equalled 0.8) which implied good correlation between results of the model calculations and the laboratory tests.

The dependence described by the wear model was expressed by means of the following formula:

$$\frac{Z}{l} = 1,13 \cdot 10^{-5} \left(\frac{p_0}{H_1}\right) \cdot \left(\frac{H_2}{H_1}\right)^{2,69} \mu^{3,23} \tag{11}$$

The wear model coefficients provided in Table 2 and in formula (11) were established for pressure p_0 expressed in [MPa].

4. Conclusions

In the friction pair components studied, the surface layer properties depend on the graphite size and arrangement as well as the structure of the matrix usually composed of martensite and retained austenite. Fractions of these components are decisive for the surface layer hardness as well as the internal stresses which may contribute to the surface layer fatigue cracking by decreasing the number of cycles necessary for it to be initiated. In such a case, the fatigue wear intensity of a cam's surface layer may be considerably increased compared to its abrasive wear intensity, which may subsequently contribute to excessive occurrence of the phenomenon in question. The most relevant technological reasons for excessive wear of friction pair components are related to the operations of heat treatment and mechanical finishing. Nonconformity with the required heat treatment parameters may cause a decrease of the surface layer hardness and an increase of abrasive wear. Certain impact may also be exerted by what is referred to as grinding cracks occurring during poor quality grinding. They can initiate fatigue cracks which, after a short period of propagation, cause rifts and excessive fatigue wear.

References

[1] A. Vadiraj, M. Kamaraj V.S. Sreenivasan, Wear and friction behavior of alloyed gray cast iron with solid lubricants under boundary lubrication, Tribology International 44 (2011) 1168-1173.

[2] W. Zwierzycki et al., Selected problems of material wear in slide friction pairs, PWN, Warsaw-Poznań, 1990 (in Polish).

[3] I. Garbar, Microstructural changes in surface layers of metal during running-in friction processes, Meccanica 36 (2001) 631-639.

[4] Yan-qiu Xia, Wei-min Liu, Qun-ji Xue, Friction and wear behavior of nodular cast iron modified by a laser micro-precision treatment sliding against steel under the lubrication of liquid paraffin containing various additives, Wear 253 (2002) 752-758.

[5] P. Adamiec, K. Witaszek, M. Witaszek, Z. Stanik, Studies of wear of nodular cast iron, Scientific Booklets of the Silesian University of Technology, Transport 39, 1999.

[6] J. Łabaj, B. Oleksiak, G. Siwiec, Analysis of the options of copper removal from liquid iron by evaporation, Metalurgija 50/3 (2011) 173-175.

[7] J. Łabaj, G. Siwiec, B. Oleksiak, Surface tension of expanded slag from steel manufacturing in electrical furnace, Metalurgija 50/3 (2011) 209-211.

[8] R. Burdzik, Z. Stanik, J. Warczek, Method of assessing the impact of material properties on the propagation of vibrations excited with a single force impulse, Archives of Materials and Metallurgy 57/2 (2012) 409-416.

[9] E. Jamro, M. Wielgosz, S. Bieniasz, W. Cioch, FPGA - ARM heterogeneous system for high speed signal analysis, Solid State Phenomena 180 (2012) 207-213.